Science in China Series B: Chemistry

www.scichina.com
chem.scichina.com
www.springerlink.com

Disclination and molecular director studies on bowlic columnar nematic phase using mosaic-like morphology decoration method

DONG YanMing†, CHEN DanMei, ZENG ErMan, HU XiaoLan & ZENG ZhiQun

Department of Materials Science and Engineering, College of Materials, Xiamen University, Xiamen 361005, China

Two bowlic cyclotriveratrylene CTV-1 and CTV-2, with different peripheral groups of —OCH_3 and —OCH_2CH_3 for CTV-1 and —OCH_3 and —OCH_2COOCH_3 for CTV-2, respectively, were synthesized by typical trimerization via a multistep sequence from vanillin. Both bowlic CTV molecules were thermotropic liquid crystals, and presented typical grainy textures of the nematic phase and homogeneous texture of the single domain nematic phase. It is of interest to observe the regular and beautiful mosaic-like morphologies after cooling from liquid crystalline phases, which appeared and vanished repeatedly in several circles of cooling and heating. The size of each mosaic was several dozens of micron. In nature, the mosaic-like morphologies are the optical pattern of cracks formed by the shrinking, due to the crystallization of frozen texture of nematic phases. By means of scanning electron microscopy, the mosaic-like morphologies were observed to consist of lamellae, and each mosaic is a rectangular multi-layer lamella, which is composed of packed single-layered lamellae. The fibrils in the diameter of about 1 μm were observed, which are the structural units of lamellae and would be the bundles of the bowlic molecular columns. The mosaic-like morphologies decorate the bowlic molecular columnar nematic phase, therefore, a novel mosaic-like morphologies decoration method was applied to reveal the director distribution of several kinds of point disclinations, such as s = +1(δ=0° and δ =90°) and s = ±1/2, and Nèel domain walls. It was shown that the bowlic molecular columnar nematic phase behaved as normal nematic phases; however, the basic structural units ordered were the bowlic molecular column or the bundles of bowlic molecular column (i.e. fibrils), but not the bowlic molecules themselves. The bowlic molecular columns acted as the rod-like molecules in a normal nematic phase. Therefore, a new term B_{CN} (bowlic columnar nematic phase) is used to describe the anomalous nematic phase in this paper.

CTV bowlic molecules, thermotropic liquid crystals, bowlic columnar nematic phase B_{CN}, mosaic-like morphologies, disclination

1 Introduction

As early as in 1980 s, Lin proposed the concept of bowlic liquid crystals[1, 2]. In 1985, Zimmermann et al.[3] and Malthête et al.[4] synthesized the rigid liquid crystalline molecules based on cyclotriveratrylene (CTV) with pyramide-shape or cone-shape successfully. The liquid crystalline molecules with these shapes are called bowlic (bowl-like) liquid crystalline molecules in this paper.

According to molecular shape, liquid crystal can be classified into rod-like, disk-like and bowlic patterns. The bowlic molecules including CTV (or TBCN, tribenzocyclononenen), CTTV (cyclotetraveratrylene), calix[n]arene, etc. have been well reviewed[5]. Although

Received September 25, 2008; accepted October 24, 2008
doi: 10.1007/s11426-009-0036-9
†Corresponding author (email: ymdong@xmu.edu.cn)
Supported by the National Natural Science Foundation of China (Grant No. 20774077), the Natural Science Foundation of Fujian, China (Grant Nos. E0510003 & E0710025) and the Project of Science and Technology of Xiamen, China (Grant No. 3502Z20055013)

all these three dimensional molecules are able to form columnar liquid crystalline phases (Figure 1), only CTV can keep bowlic structure in columnar liquid crystalline phases [6].

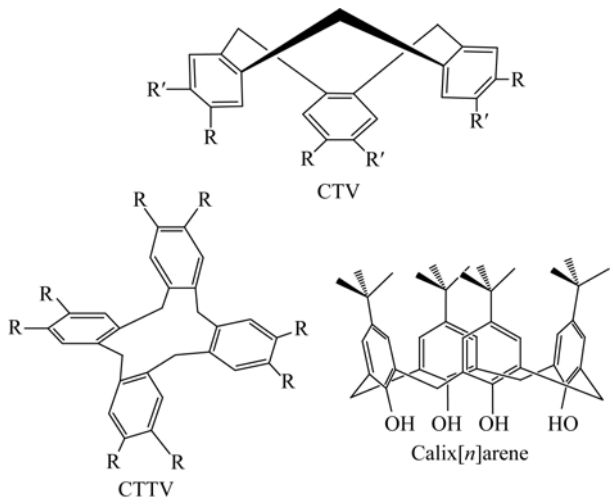

Figure 1 Three kinds of bowlic molecules to be able to form columnar liquid crystalline phases.

Lindsey et al.[7] and Hyatt et al. [8] have reported the synthesis methods of this kind of molecule in the 1960's and 1970's of the 20th century respectively. However, Zimmermann et al.[3] and Malthête et al.[4] reported the liquid crystalline behavior of bowlic molecules CTV until 1985.

In addition to liquid crystalline behavior, CTV and its derivatives also have some important properties, such as optical activity and chirality[9–12]. In supramolecular chemistry, CTVs are macrocyclic host molecules which can form cavity host-guest complex macromolecule with metal ions and organometallic complex, etc. [13–20]. This kind of molecule with special shape has some special applications.

CTV is a kind of circle trimer, with bowlic structure and high rigidity[21]. This topological structure is very easy to self-assemble into stable columnar structure. Although some researches of liquid crystalline behavior of bowlic molecules have been reported, but there have been no studies about their texture, disclination and director distribution.

Normally, the nematic texture observed under polarized optical microscopy (POM) is an optical effect of disclination, which is not the real morphology of disclination. So far, it is impossible to observe the morphology of disclination and the director distribution nearby directly by experiments. The only way people can adopt is indirect, that is, using all kinds of decoration techniques. Chen et al.[22] reviewed three determination techniques, including lamellar decoration, banded texture decoration and surface crack decoration. For example, Windle et al.[23] observed the lamellae in the nematic texture of aromatic copolyester B-N (i.e. Vectra) after slow cooling, and the lamellae were studied by means of scanning electron microscopy (SEM) and transmission electron microscopy (TEM). Still further, Dong et al.[24] detected the disclinations with $s = -1/2$ and $s = +1$ and their director distribution under SEM by using the decoration technique of these lamellae and etching technique. Chen et al. [22, 25] reported firstly the banded texture decoration technique, and the nematic Schlieren texture of aromatic copolyester was decorated by banded texture, which was induced during cure. The disclinations with $s = \pm 1/2$, $s = \pm 1$ and $s = -3/2$, and inverse wall were studied using POM. Wang et al.[26] determined the disclinations with $s = \pm 1/2$ and $s = +1$ in the lyotropic mesophase of polydiacetylene/chloroform solution using surface crack decoration technique. A stripe texture observed over large regions of the solid film is suggested to be a decoration effect due to internal stress as a result of solvent evaporation when the films are prepared by solution casting.

Two bowlic molecules, i.e. CTV-1 and CTV-2, with peripheral alkoxyl groups are synthesized in this paper. The interesting mosaic-like morphologies were firstly observed in the liquid crystalline textures. A novel mosaic-like morphologies decoration technique was developed to observe the disclinations and director distribution. This technique is different from both lamella decoration technique and surface crack decoration technique mentioned previously. It is an organic combination of these two techniques. Using this new technique, the disclinations and the director distribution nearby in a new nematic phase, i.e., the columnar nematic phase of bowlic molecules, were revealed.

2 Experimental

2.1 Materials and instrument

All reagents and solvents were of analysis reagent (AR) or chemical purity (CP). The solvents were purified by distilling before use. The thin layer chromatography

(TLC) silica gel H (type 60, CP, made in YanTai ZiBu Huangwu Silica Gel Factory) was used for the separation and purification of products. Nuclear magnetic resonance spectrometer (Bruker AV400 NMR), mass spectrometer (Bruker Dalton Esquire 3000 plus), element analyzer (Carlo Erba 1110 CHNS-O), differential scanning calorimetry (DSC, Netzsch DSC204), with both heating rate and cooling rate being 10℃/min, Mettler FP90 hot stage coupled polarized optical microscope (Nikon Eclipse ME600), and scanning electron microscope (XL30 ESEM) were employed. The silica gel plate HS2GF25 (thickness: 0.20－0.30 mm, made in YanTai ZiBu Huangwu Silica Gel Factory) was used in TLC, and iodine gas was used to dye after the separation was over.

2.2 Synthesis and structure characterization

We prepared two CTV derivatives from vanillin by referring to refs. [27, 28]. The synthesis route designed and structure characterization of products are as follows.

The formulas and synthesis routes of intermediate **1**, intermediate **2** and product CTV-1 are shown in Figure 2. For **3**, **4**, and CTV-2 are shown in Figure 3.

2.2.1 4-ethoxy-3-methoxybenzaldehyde **1**. A mixture of acetone (250 mL), vanillin (15.2 g, 100 mmol), K_2CO_3 (14.5 g, 105 mmol) and bromoethane (7 mL, 95 mmol) was refluxed in a 500 mL round bottom flask for 24 h followed by removing acetone by rotary evaporation. The residue was redissolved in $CHCl_3$ (100 mL), filtered, dried over by anhydrous $MgSO_4$ and after collection by rotary evaporation, recrystallized from hexane to give **1** as a light yellow solid (13.4 g, yield: 78%).

^{1}H NMR ($CDCl_3$, 400 MHz): 1.54 (t, 3H, *J*=7.2 Hz, C$\underline{H}_3$), 3.96 (s, 3H, C$\underline{H}_3$OAr), 4.21－4.23 (m, 2H, C$\underline{H}_2$OAr), 6.98 (d, *J*=8.4 Hz, 1H, ArC$\underline{H}$), 7.44 (d, *J*=8.4 Hz, 1H, ArC$\underline{H}$), 7.48 (s, 1H, ArC$\underline{H}$), 9.87 (s, 1H, C$\underline{H}$O); ^{13}C NMR ($CDCl_3$, 100 MHz): 14.7 ($\underline{C}H_3$), 55.9 ($\underline{C}H_3$OAr), 64.7 ($\underline{C}H_2$OAr), 109.7, 111.8, 126.6 (Ar$\underline{C}$H), 130.3 (Ar$\underline{C}$CHO), 150.1 (Ar$\underline{C}$OCH$_3$), 154.3 (Ar-$\underline{C}$OCH$_2$), 190.8 ($\underline{C}$HO); Anal. Calc. for $C_{10}H_{12}O_3$: C, 66.65; H, 6.71, Found: C, 66.53; H, 6.95; MS (ESI$^+$, *m*/z) 180.2(M+Na$^+$, calc. 203.2).

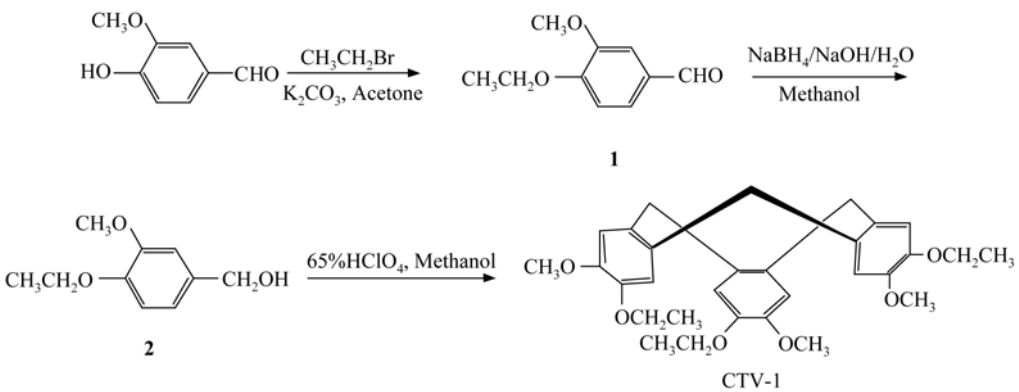

Figure 2 The formulas and synthesis routes of intermediate **1**, intermediate **2** and product CTV-1.

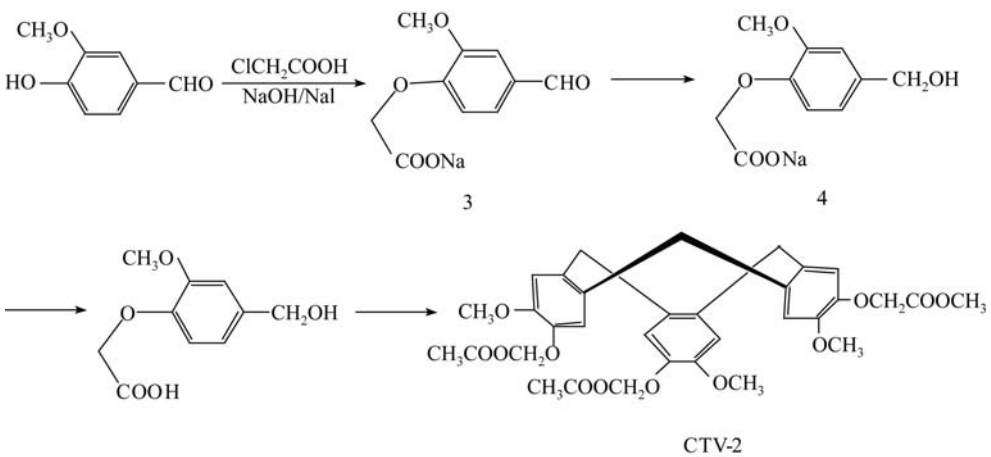

Figure 3 The formulas and synthesis routes of intermediate **3**, intermediate **4** and CTV-2.

2.2.2 4-ethoxy-3-methoxybenzylalcohol **2**. An aqueous NaOH solution containing H_2O (60 mL), NaOH (0.75 g, 18.8 mmol), and $NaBH_4$ (3.32 g, 79.3 mmol) was added into a 250mL methanol solution of **1** (13.5 g, 75 mmol) containing H_2O (60 mL), NaOH (0.75 g, 18.8 mmol), and $NaBH_4$ (3.32 g, 79.3 mmol) dropwise through an additional funnel. The mixture was stirred with a Teflon-coated magnetic stirrer for 4 h at room temperature, followed by removing methanol by rotary evaporation, and then diluted with water (200 mL), and acidified with 5% HCl. The organic material was extracted with dichloromethane. The organic layer was thoroughly washed with water to neutral and dried over anhydrous $MgSO_4$ resulting in **2** after rotary evaporation as a white solid (12.6 g, yield: 92%).

^{1}H NMR ($CDCl_3$, 400 MHz): 1.45 (t, *J*=7.2 Hz，3H, C$\underline{H}_3$), 3.87 (s, 3H, C$\underline{H}_3$OAr), 4.10 (t, *J*=6.8 Hz, 2H, C$\underline{H}_2$OAr), 4.61 (s, 2H, C$\underline{H}_2$OH), 6.85 (d, *J*=8.0 Hz, 1H, Ar C$\underline{H}$), 6.92 (d, *J*=8.0 Hz, 1H, ArC$\underline{H}$), 6.98 (s, 1H, ArC$\underline{H}$); ^{13}C NMR ($CDCl_3$, 100 MHz): 14.5 (C$\underline{H}_3$), 55.5 (C$\underline{H}_3$OAr), 64.1 (C$\underline{H}_2$OH), 64.5(C$\underline{H}_2$OAr), 110.3, 112.2, 119.1 (ArC$\underline{H}$), 137.9 (ArC$\underline{C}$H$_2$OH), 149.0 (ArC$\underline{C}$OCH$_3$), 149.8 (ArC$\underline{C}$OCH$_2$); Anal. Calc. for $C_{10}H_{14}O_3$: C, 65.91; H, 7.74, Found: C, 65.82; H, 7.90; MS (ESI$^+$, *m*/*z*) 182.2 (M+Na$^+$, calc. 205.3).

2.2.3 (±) 2,7,12-tris-methoxy-3,8,13-tris-ethoxy-10, 15-dihydro-5H-tribenzo-[a, d, g]cyclononene (CTV-1). To a solution of 100 mL methanol and **2** (5.46 g, 30 mmol) in a 500 mL round bottom flask containing a Teflon-coated magnetic stirrer, was added 50 mL 65% $HClO_4$ through an addition funnel at ice-water bath temperature. The resulting pink or purple solution was stirred for 24 h at room temperature, affording a whitish crystalline precipitate. 100 mL water was added dropwise with shaking, and the solution turned light yellow by being alkalized with 10% NaOH (Caution: all the perchloric acid must be removed at this step). The resulting precipitate was collected by suction filtration and washed with H_2O to be neutral, then purified by Soxhlet immersion and extracted in diethyl ether. Finally, CTV-1 was obtained as a white solid (2.12 g, yield: 43%).

^{1}H NMR ($CDCl_3$, 400 MHz): 1.41 (t, 9H, *J*=9.2 Hz, C$\underline{H}_3$), 3.56 (d, 3H, *J*=13.6 Hz, ArHaC$\underline{H}$eAr), 3.54 (s, 9H, C$\underline{H}_3$OAr), 4.06－4.10 (m, 6H, *J*=7.2 Hz, C$\underline{H}_2$OAr), 4.75 (d, 3H, *J*=13.6 Hz, Ar$\underline{H}$aCHeAr), 6.84 (s, 3H, ArC$\underline{H}$), 6.86 (s, 3H, ArC$\underline{H}$); ^{13}C NMR ($CDCl_3$, 100MHz): 14.9 (C$\underline{H}_3$), 36.5 (ArC$\underline{H}_2$Ar), 56.1 (C$\underline{H}_3$OAr), 64.5 (C$\underline{H}_2$OAr), 113.5, 114.9 (ArC$\underline{H}$), 131.9 (ArC$\underline{C}$H$_2$), 146.9, 148.1 (ArC$\underline{C}$O); Anal. Calc. for $C_{27}H_{12}O_3$: C, 64.27; H, 7.19, Found: C, 64.22; H, 7.30; MS (ESI$^+$, *m*/*z*) 492.3 (M+Na$^+$, calc. 510.2).

2.2.4 4-formacyl-2-methoxyphenoxy acetic acid, and sodium salt **3**. A stirred solution of chloroacetic acid (18.9 g, 0.20 mol) in ethanol (300 mL) was neutralized with 20 mL 35% aqueous NaOH, to which were successively added 27.4 g vanillin (0.18 mol), 20 mL 35% aqueous NaOH and sodium iodide (0.28g). The mixture was refluxed for 5 h under nitrogen. After cooling to room temperature, they were kept at 4°C for 15 h. The resulting precipitate was filtered off, washed with little ethanol, recrystallized from 80 mL of hot water and dried under vacuum to afford a light yellow solid **3** (29.3 g, yield: 70%).

^{1}H NMR (D_2O, 400 MHz): 3.62 (s, 3H, OC$\underline{H}_3$), 4.41 (s, 2H, OC$\underline{H}_2$), 6.73 (d, 1H, *J* = 8.4 Hz, ArC$\underline{H}$), 7.16 (s, 1H, ArC$\underline{H}$), 7.31 (d, 1H, *J* = 9.6 Hz, ArC$\underline{H}$), 9.49 (s, 1H, C$\underline{H}$O); ^{13}C NMR (D_2O, 100 MHz): 55.5 (O$\underline{C}$H$_3$), 66.9 (O$\underline{C}$H$_2$), 109.8, 111.6, 127.5, 129.2, 148.3, 152.9 (Ar$\underline{C}$H), 175.6 ($\underline{C}$O$_2$), 194.5 ($\underline{C}$HO). Anal. Calcd. for $C_{10}H_9O_5Na$.: C, 51.73; H, 3.91. Found: C, 51.87; H, 4.02. MS (ESI$^+$, *m*/*z*) 232.2 (M+Na$^+$, calc. 255.2).

2.2.5 4-hydroxymethyl-2-methoxyphenoxy acetic acid, and sodium salt **4**. An aqueous NaOH solution containing H_2O (60 mL), NaOH (0.75 g, 18.8 mmol), and $NaBH_4$ (3.00 g, 79.3 mmol) was added into a 250 mL CH_3OH solution of **3** (17.4 g, 75 mmol) dropwise through an additional funnel. The mixture was stirred with a Teflon-coated magnetic stirrer for 4 h at room temperature, then collected by rotary evaporation, and recrystallized three times from hot water and dried under vacuum to afford a white solid **4** (16.8 g, yield: 96%).

^{1}H NMR (D_2O, 400 MHz): 3.78 (s, 3H, OC$\underline{H}_3$), 4.36 (s, 2H, C$\underline{H}_2$OH), 4.45 (s, 2H, OC$\underline{H}_2$CO$_2$), 6.70 (d, 1H, *J* = 8.0 Hz, ArC$\underline{H}$), 6.82 (dd, 1H, *J* = 8.0 and 1.6 Hz, ArC$\underline{H}$), 6.94 (d, 1H, *J* = 1.6 Hz, ArC$\underline{H}$); ^{13}C NMR (D_2O, 100 MHz): 56.2 (O$\underline{C}$H$_3$), 64.9 ($\underline{C}$H$_2$OH), 68.8 ($\underline{C}$H$_2$CO$_2$), 111.5, 113.5, 120.7, 136.3, 147.4, 149.7 (Ar$\underline{C}$H), 175.6 ($\underline{C}$O$_2$). Anal. Calcd. for $C_{10}H_{11}O_5Na$: C, 51.29; H, 4.73. Found: C, 51.38; H, 4.95. MS (ESI$^+$, *m*/*z*) 234.2 (M+Na$^+$, calc. 257.3).

2.2.6 (±)2,7,12-tris(methoxycarbonylmethoxy)-3,8,13-trimethoxy-10,15-dihydro-5H-tribenzo-[a,d,g]cyclononene (CTV-2). Alcohol **4** (10 g, 42.7 mmol) was added portionwise to 150 mL 65% aqueous perchloric acid and the resulting solution was stirred at room temperature for 18 h. Then, 1 L of a chilled 1:9 acetic acid-water mixture

was added dropwise. The resulting precipitate was collected by slow suction filtration and washed with acetic acid (200 mL) and water (200 mL). The still wet and acidic cake was added to a mixture of methanol (240 mL) and methyl orthoformate (120 mL), and the resulting suspension was refluxed for 5 h, and the acid slowly dissolved while a precipitate began to form. The reaction mixture was kept for 2 days at −20℃ and the solid was collected by suction filtration. This crude product was purified by chromatographed silica gel by using dichloromethane-diethyl ether 9∶1 (*v*/*v*) as the eluant, and dried under vacuum for 5 h to give 3.5 g CTV-2 as a white crystalline powder (yield: 37%).

^{1}H NMR ($CDC1_3$, 400 MHz): 3.42 (d, 3H, J = 13.6 Hz，ArHaC<u>H</u>eAr),), 3.80 (s, 9H, $CO_2C\underline{H}_3$), 3.88 (s, 9H, $OC\underline{H}_3$), 4.03－4.09 (m, 6H, $OC\underline{H}_2$), 4.58 (d, 3H, J = 13.6 Hz, Ar<u>H</u>aCHeAr), 6.78 (s, 3H, ArC<u>H</u>), 6.87 (s, 3H, ArC<u>H</u>) ; ^{13}C NMR ($CDCl_3$, 100MHz): 36.4 ($Ar\underline{C}H_2Ar$), 52.1 ($O\underline{C}H_3$), 56.0 ($CO_2\underline{C}H_3$), 67.3 ($O\underline{C}H_2$), 113.7, 117.6, 131.5, 134.1, 145.9, 148.6 (Ar<u>C</u>H), 169.9 ($\underline{C}O_2$). Anal. Calcd. for $C_{33}H_{36}O_{12}$: C, 63.45; H, 5.81. Found: C, 63.32; H, 5.90. MS (ESI^+, *m*/*z*) 624.63 ($M+Na^+$, calc. 647.8).

3 Results and discussion

3.1 Appearance of mosaic-like morphologies

Both CTV-1 and CTV-2 were thermotropic liquid crystals. Their structure difference is that the peripheral groups of the former are larger than the latter, therefore, the latter has poorer structure symmetry (i.e. larger difference between R and R′ in CTV structure in Figure 1) and poorer molecular rigidity, which causes the poorer liquid crystallinity and demonstrates a more narrow liquid crystal temperature region. The DSC traces and the data of melting point T_m, clearing temperature T_c, and liquid crystal temperature region ΔT are shown in Figure 4 and Table 1.

The joint point of these two CTV derivatives is that no intermolecular hydrogen bonds could be formed, so the interactions between molecules are weak. Therefore, their liquid crystalline textures were very similar. A typical nematic texture, the grainy texture, was found when heating or cooling to the liquid crystalline state (Figure 5(a) and (c)). At some sites, single domains with round or oval shape and homogeneous birefringence can be found (Figure 5(b) and (d)). The single domains and the grainy textures occurred simultaneously, because both of them are of nematic texture. The single domain is also named homogeneous texture, which is the result of homogeneous alignment of director.

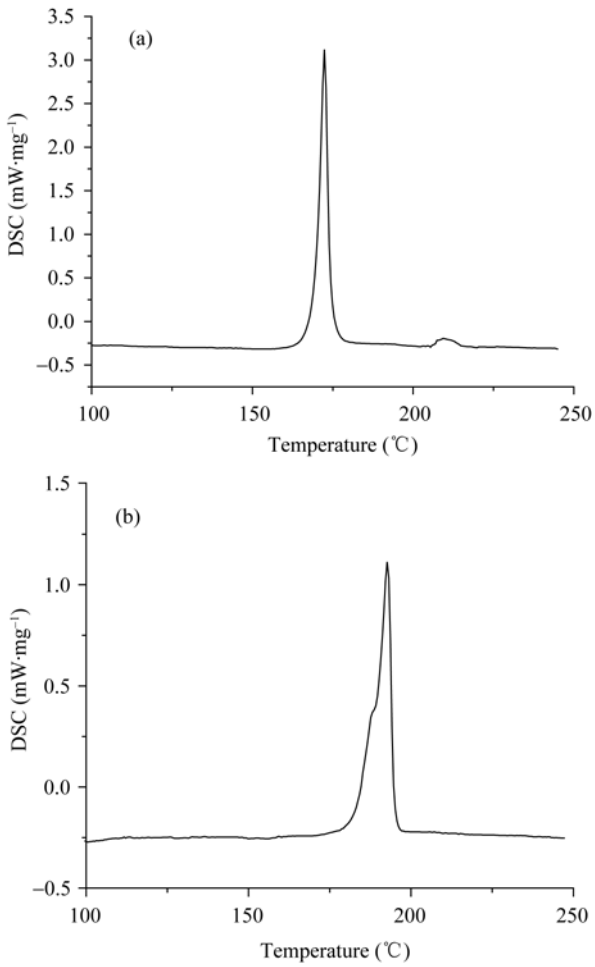

Figure 4 The DSC traces of CTV-1 (a) and CTV-2 (b)

Table 1 The peripheral group and liquid crystalline transition temperature of CTV derivatives

	CTV-1	CTV-2
R	OCH_3	OCH_3
R′	OCH_2CH_3	OCH_2COOCH_3
T_m (℃)	169	187
T_c (℃)	207	192
ΔT (℃)	38	5

It is of interest to find very beautiful mosaic-like morphologies in domains with larger size while cooling from mesophase. The Mosaics were quite regular, the length and width were about several dozens of μm (Figure 6). After several circles of heating and cooling from mesophase to room temperature, Mosaic-like morphologies can reappear, but the size became smaller, and the arrangement became more and more irregular (Figure 7).

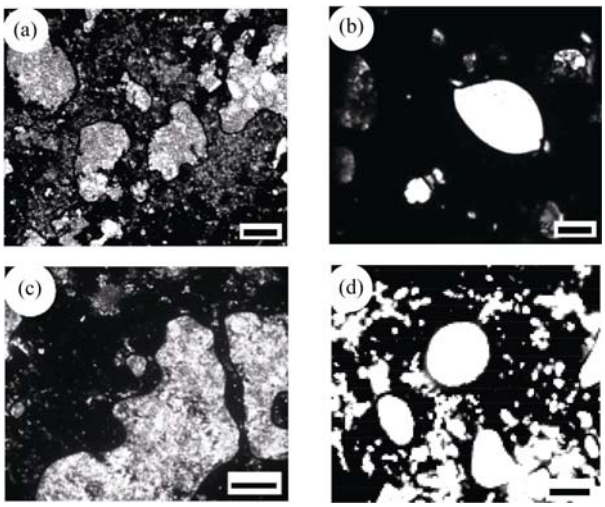

Figure 5 Two kinds of nematic textures under hot-stage coupled POM. (a) The grainy texture of CTV-1, at 170℃; (b) the homogeneous texture of CTV-1, at 120℃; (c) the grainy texture of CTV-2, at 189.6℃; (d) the homogeneous texture of CTV-2, at 191.2℃. The scales in (a), (b) and (c) all are 200 μm, but the scale in (d) is 150 μm .

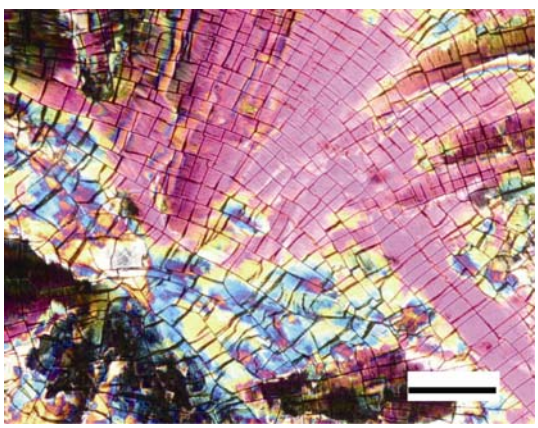

Figure 6 The POM photograph of mosaic-like morphologies of CTV-1 after a circle of heating and cooling. The scale is 100 μm.

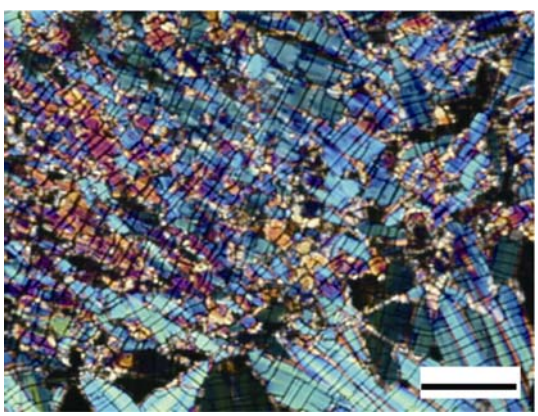

Figure 7 The POM photograph of mosaic-like morphologies of CTV-1 after three circles of heating and cooling. The scale is 100 μm.

The generation process of the mosaic-like morphologies in a piece of single domain of CTV-1 was firstly studied upon a hot stage-coupled POM (Figure 8). It is found that the single domain cracked along two mutually perpendicular directions from the edge toward the inside. One direction was the preferred direction of the cracks, which penetrated from one end to the other end and was called "main cracks". The cracks on another direction were shorter, called "vertical cracks". After cooling further, the cracks formed completely, the final mosaic-like morphologies appeared. Because the boundary of the lamellae was the mechanical weak point, the cracks almost occurred on every boundary. Therefore, the cracks delineated the morphologies of the lamellae, each piece of mosaic was a piece of lamella. The appearance of mosaic-like morphologies was later than that of nematic textures at the cooling run from clear temperature. However, the vanish of mosaic-like morphologies was earlier than that of nematic textures at the second heating run from room temperature to melting points. It can be concluded that the appearance of mosaic-like morphologies is the result of crystallization. The crystallization is a process with density increasing, and the volume shrinks, that causes the fractures. It is unusual to find obvious cracks for normal liquid crystalline molecules during cooling and crystallization. It implies that there was larger volume shrinking during crystallization for bowlic liquid crystals. This behavior of bowlic liquid crystals can be explained by much tighter packing during self-assembling into columns.

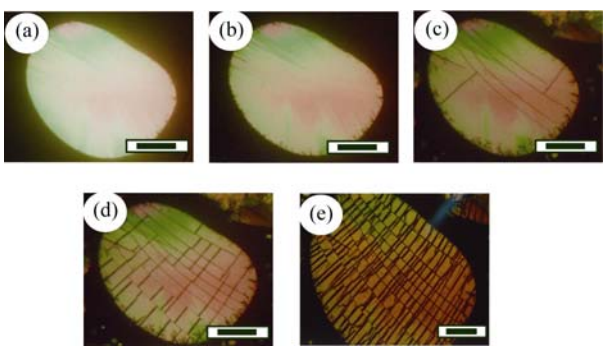

Figure 8 POM photographs of the dynamic process forming mosaic-like morphologies of CTV-1 observed under hot-stage-coupled POM at different temperatures of first cooling from clear temperature. (a) 160℃, (b) 130℃, (c) 115℃, (d) 85℃ and (e) room temperature. The scale is 100 μm .

The X-ray diffraction was applied to prove that mosaic-like morphologies are crystal morphologies, but not liquid crystal texture. The X-ray diffraction diagrams of

CTV-1 and CTV-2 with mosaic-like morphologies are shown in Figures 9 and 10 respectively. Many sharp diffraction peaks occurred at wide angles, indicating that the crystals have been formed upon the basis of original nematic texture.

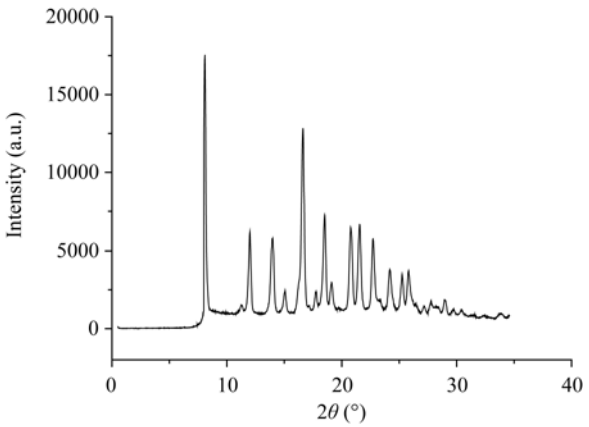

Figure 9 The X-ray diffraction diagram of mosaic-like morphologies of CTV-1.

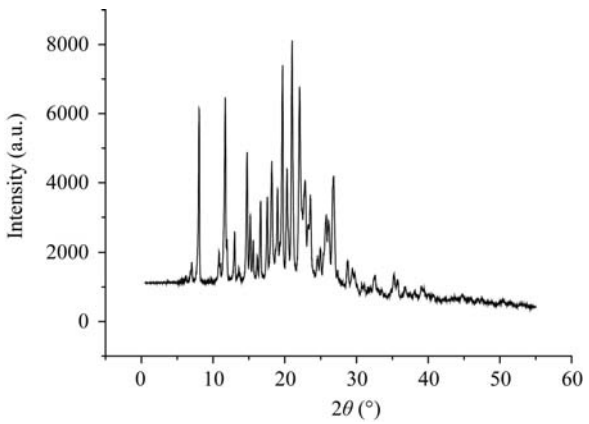

Figure 10 The X-ray diffraction diagram of mosaic-like morphologies of CTV-2.

3.2 The details of mosaic-like morphologies under SEM

Figures 11 and 12 are SEM photographs of mosaic-like morphologies of CTV-1 after one and three circles of heating and cooling respectively. The mosaics were regularly arranged along two directions, which were cross basically. As shown in Figure 10(b), the main cracks were in the horizontal direction, which continued from left to right. On the other hand, the so-called vertical cracks were in the perpendicular direction, whose order was lower than that of the main cracks. The average size of mosaics of CTV-1 read after a circle of heating and cooling was about (40—80 μm)× (20—40 μm). But the average size of mosaics of CTV-1 read after three circles of heating and cooling was about (10—30 μm)× (10—20 μm). The average size of mosaics decreased after several circles of heating and cooling, moreover, the size became less uniform. The order of both directions also decreased, especially the vertical cracks almost lost the order. The mosaics also became more uneven in the third dimensional direction vertical to the paper. It can be explained by the accumulation history effect of defects. Some parts of crystalline defects remained to the mesophase during heating, subsequently some parts of mesophase defects remained back to the crystal during cooling of the circle.

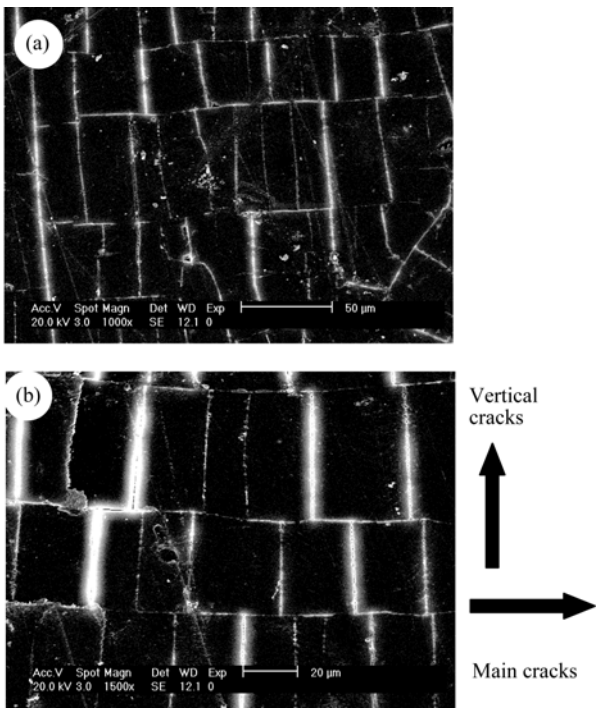

Figure 11 The SEM photographs of mosaic-like morphologies of CTV-1 after a circle of heating and cooling.

From the SEM photographs, it can be seen directly that the mosaic-like morphologies were formed by cracks, the bright stripes were just these cracks. Another fact to prove the existence of the cracks was presented by peeling technique. During the preparation of SEM samples, some of the mosaics were stripped off while peeling off the cover glass slides (Figures 13 and 14). The cracks can be seen to penetrate the whole thickness, and each mosaic peeled was just a single lamella. The internal structure can be studied through the edge regions of these mosaics peeled, and then the forming mechanism could be deduced from the structure. There are two experimental techniques that can be used to increase the anatomical effect, i.e., tilting the sample and shearing the sample.

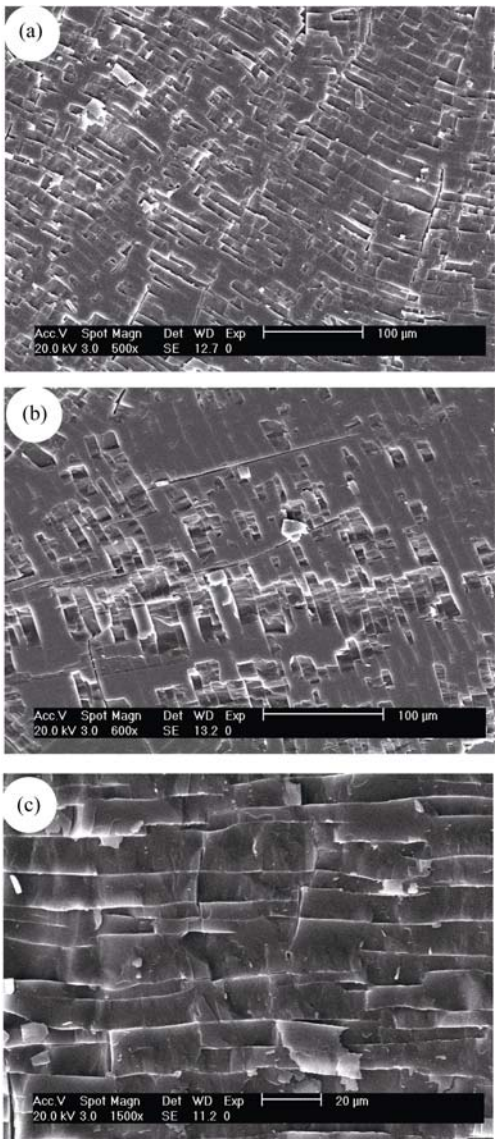

Figure 12 The SEM photographs of mosaic-like morphologies of CTV-1 after three circles of heating and cooling.

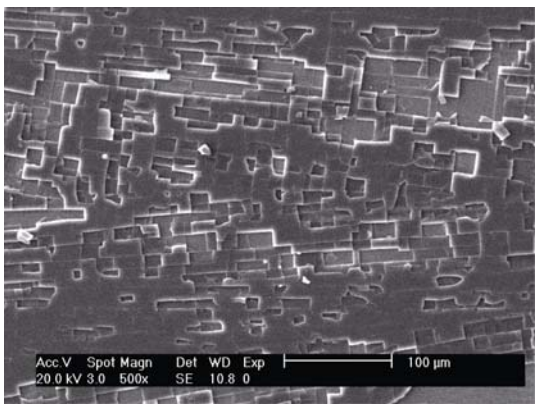

Figure 13 The SEM photograph of mosaic-like morphologies of CTV-1 with parts of mosaics stripped.

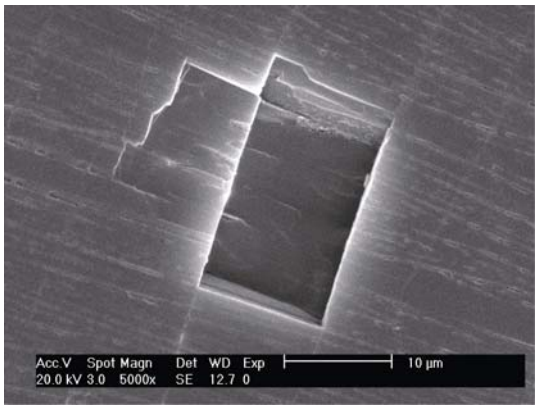

Figure 14 The SEM photograph of mosaic-like morphologies of CTV-2 with a piece of mosaic stripped.

(1) Tilted sample

When the SEM samples of CTV-1 were tilted at 30°, the microstructures are shown in Figure 15(a) and (b). From the cracks, it can be seen that every mosaic had

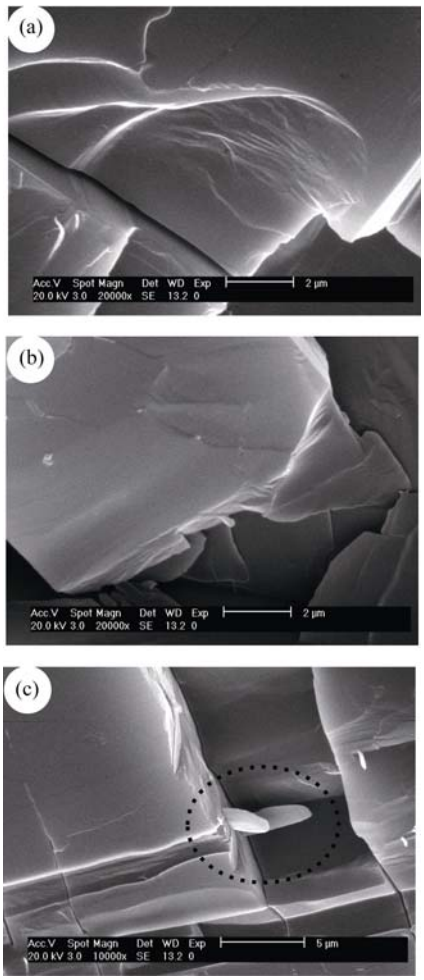

Figure 15 The SEM photograph of internal structure in mosaic-like morphologies of the tilted CTV-1 sample.

multi-layer lamellar structure. The thickness of a single layer of lamella was measured to be about 1 μm. From Figure 15(c), it can also be seen clearly that some fibrils were drawn out, the diameter of which was also about 1 μm. It implied that the single layer of lamella consists of the fibrils. What is the composition of the fibril? The reasonable inference is that a fibril is a bundle of bowlic molecular columns. The bowlic molecules tend to form the column and further aggregate to form the bundle of columns, due to the strong driving force of self-assembling. These fibrils were observed to be vertical to the direction of the main cracks, i.e. parallel to the vertical cracks.

(2) Sheared sample

The SEM samples of CTV-1 were shorn at the temperature region of liquid crystal, and then cooled, and the broken mosaic-like morphologies are shown in Figure 16. No preferred orientation of sub-structure was observed. Some ribbons consisting of lamellae without cracks were observed (Figure 17(a)). Rectangular teeth can be noticed at the edges of the ribbon (Figure 17(b)). They were obviously the contour of the end of the fibrils. The long side of the ribbon was main crack, so the fibrils were vertical to the main cracks.

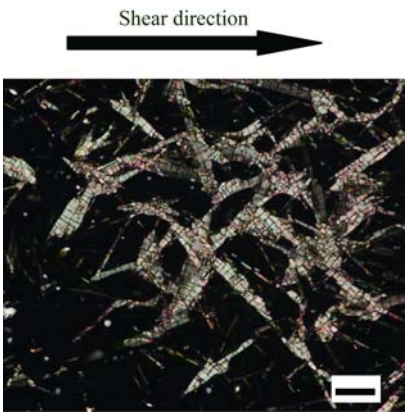

Figure 16 The POM photograph of mosaic-like morphologies of CTV-1 after shearing. The scale is 300 μm.

The phenomenon that the fibrils were vertical to the main cracks could also be verified by the birefringence symbol of the mosaic-like morphologies. By inserting a λ plate in POM, the birefringence symbol of the mosaic-like morphologies was measured (Figure 18). The color in direction of quarter 1 and quarter 3 changed from violet to blue, a higher interference color, and the color in direction of quarter 2 and quarter 4 changed from violet to yellow, a lower interference color. It means that the refraction index n of main crack direction is smaller, and the n of vertical crack direction is larger. Because the axis direction of column packed by bowlic molecules is the direction with higher atomic density, and its refraction index must be larger. In Figure 18, it can be recognized that the vertical cracks are radial, so the direction of vertical cracks was that of director. The relationship between birefringence and all sub-structures is shown in Figure 19.

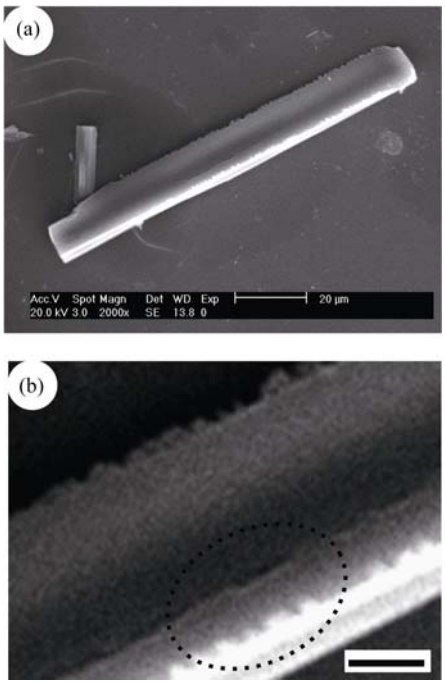

Figure 17 The ribbon structure in shorn mosaic-like morphologies of CTV-1, and (b) is the detail of (a). The scale is 4 μm for (b).

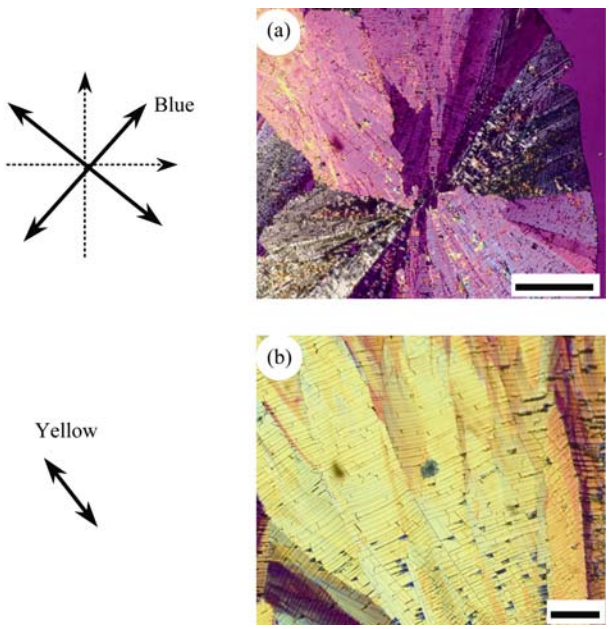

Figure 18 The interference colors of mosaic-like morphologies of CTV-1 in POM after inserting a λ plate. The scales are 500 μm.

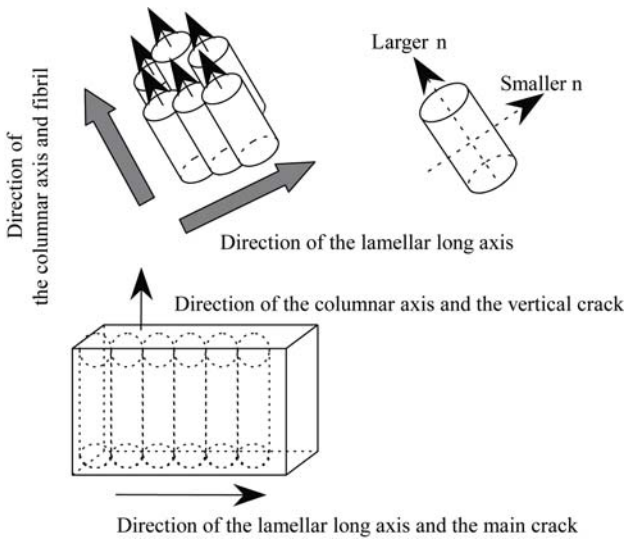

Figure 19 The illustration of optical properties of mosaic-like morphologies.

In sum, the formation process of lamellae in mosaic-like morphologies is illustrated in Figure 20. Firstly, the bowlic molecules self-assemble into columnar microstructure, and the columnar diameter is about 5 nm according to the calculation of the molecular structure. Then the columns self-assemble into fibrils with the diameter being about 1 μm along a same director. The length of fibril ranges from about 20 μm to about 40 μm, which is the same as the width of a piece of mosaic. Subsequently, the fibrils self-assemble into single layer lamellae with the size of 20 μm×100 μm×1 μm, and several single layer lamellae pack to form a multi-layer lamella, i.e. a piece of mosaic. The columnar direction (i.e. the direction of director) in mosaic is vertical to the main cracks, whose direction is the long side of mosaic.

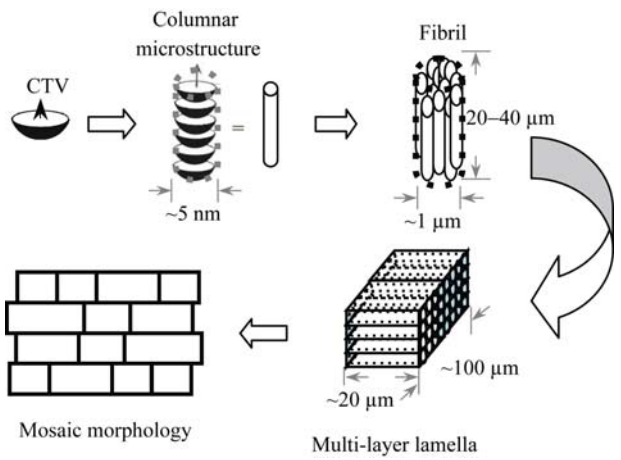

Figure 20 The illustration of self-assembling of lamellar structure.

The mosaic-like morphology formed by bowlic molecules is not equal to typical mosaic-like texture, although their names are similar. Another name of typical mosaic-like texture is marble-like texture. The direction of molecular directors in adjacent domains is often not uniform, and there are obvious boundaries between domains. However, the direction of molecular directors in adjacent mosaic is basically uniform in mosaic-like morphology. A piece of mosaic is not exactly a domain consisting of many pieces of mosaic. The direction of molecular directors varies from domain to domain. That is the reason why we can research the disclination and molecular director distribution from the morphologies.

It is more important that the composition unit of traditional mosaic-like texture is rod-like molecule, and the direction of the molecular director is rod axis. However the composition unit of mosaic-like morphologies is not bowlic molecule itself, but is bowlic molecular columns, and the direction of the molecular director is columnar axis.

3.3 The disclination and molecular director distribution of columnar nematic texture decorated by lamellae

Because the lamellae were decorated on the columnar nematic texture, the director distribution of the original columnar nematic texture could be obtained directly from the distribution map of lamellae. Several kinds of general disclinations of nematic phase can be observed, including the point disclination with the strength $s = +1$, $s = \pm 1/2$ and three-dimensional disclination Nèel domain wall. It is noticed that the direction of main crack was vertical to the molecular director, so the diagrams formed by main cracks discussed later were different from the director maps. The direction of main cracks was just vertical to the molecular directors.

3.3.1 Director distribution around the disclination with strength s=+1. The disclination with strength s=+1 and the angle between director and radius δ=0 has a director distribution map with the disclination point at the center and the directors are radial from the center. This kind of disclination was detected in both CTV-1 and CTV-2 (Figures 21, 22 and 23). The tangential direction of circle was the direction of main cracks, hence the diagrams looked like a series of concentric circles of main cracks, but the director distribution map was a series of radial directors.

Figure 21 The POM photograph of point disclination with $s = +1$ ($\delta = 0^\circ$) decorated by lamellae presented in the mosaic-like morphologies of the CTV-2 sample. The scale is 100 μm, and the director distribution map is shown on the right side.

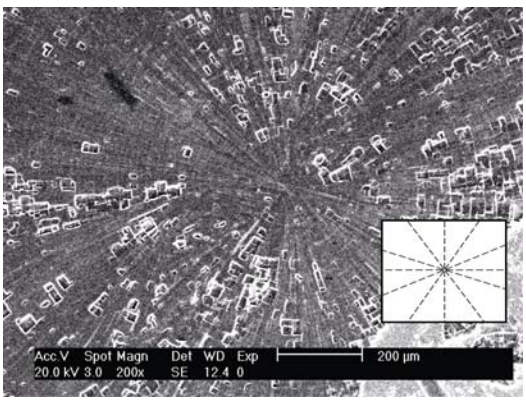

Figure 22 The SEM photograph of point disclination with $s = +1$ ($\delta = 0^\circ$) decorated by lamellae presented in the mosaic-like morphologies of the CTV-2 sample. The director distribution map is shown on the right side.

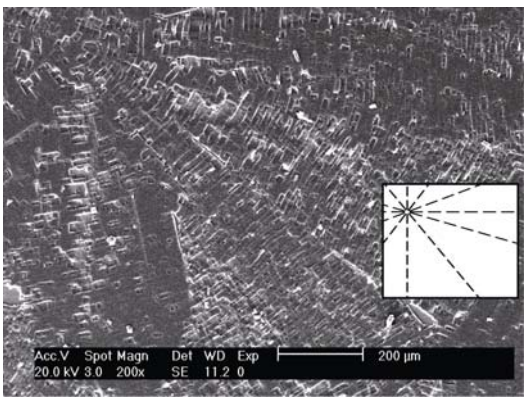

Figure 23 The SEM photograph of point disclination with $s = +1$ ($\delta = 0^\circ$) decorated by lamellae presented in the mosaic-like morphologies of the CTV-1 sample. The director distribution map is shown on the right side.

The result of Figure 24 is just opposite, i. e. the main cracks were seen to be radical, and the director is tangential. So it was the disclination with $s = +1$ and $\delta = 90^\circ$. The director distribution map looked like a series of concentric circles of directors.

3.3.2 Director distribution around the disclination with strength $s = \pm 1/2$. The disclinations with strength $s = +1/2$ or $-1/2$ were observed in CTV-1 and CTV-2. Figures 25 and 26 are the examples of disclinations with $s = +1/2$ and their director distribution maps. Figure 27 is the example of disclinations with $s = -1/2$ and its director distribution map.

3.3.3 Director distribution around the Nèel domain wall. The boundary between two domains is the site that directors turn their direction, which is termed domain walls or inverse wall. It is three-dimensional disclination. It was observed that direction of main cracks turned suddenly (Figures 28 and 29). There are two sorts

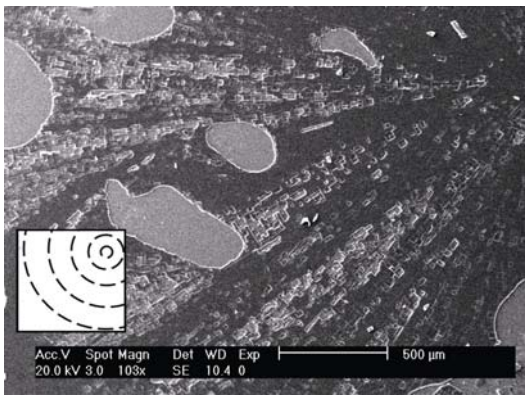

Figure 24 The SEM photograph of point disclination with $s = +1$ ($\delta = 90^\circ$) decorated by lamellae presented in the mosaic-like morphologies of the CTV-1 sample. The director distribution map is shown on the left side.

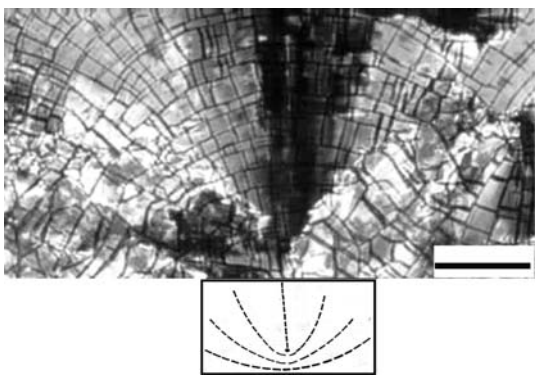

Figure 25 The POM photograph of point disclination with $s = +1/2$ decorated by lamellae presented in the mosaic-like morphologies of the CTV-1 sample. The scale is 200 μm. The director distribution map is shown below the photograph.

of domain wall, one is Nèel domain wall, another is Bloch domain wall[24]. The former is more often observed, Figure 30 shows the director distribution around a Nèel domain wall.

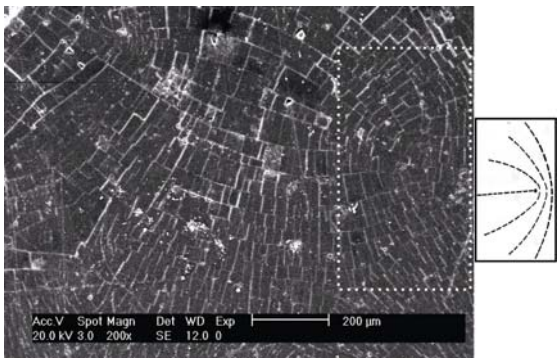

Figure 26 The SEM photograph of point disclination with s=+1/2 decorated by lamellae presented in the mosaic-like morphologies of the CTV-1 sample. The director distribution map is shown on the right side.

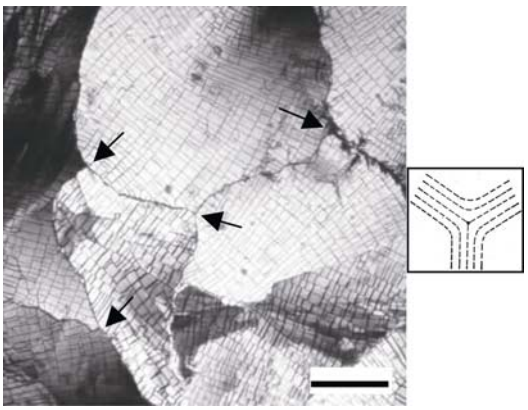

Figure 27 The SEM photograph of several point disclinations with s = −1/2 decorated by lamellae presented in the mosaic-like morphologies of the CTV-2 sample. The scale is 300 μm. The director distribution map is shown on the right side.

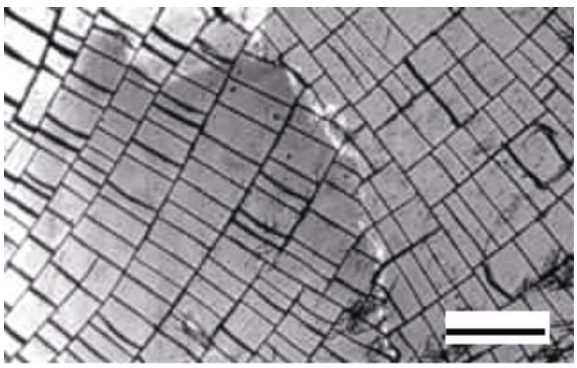

Figure 28 POM microstructure of the Nèel domain wall decorated by lamellae appearing in the mosaic-like morphologies of the CTV-1. The scale is 50 μm

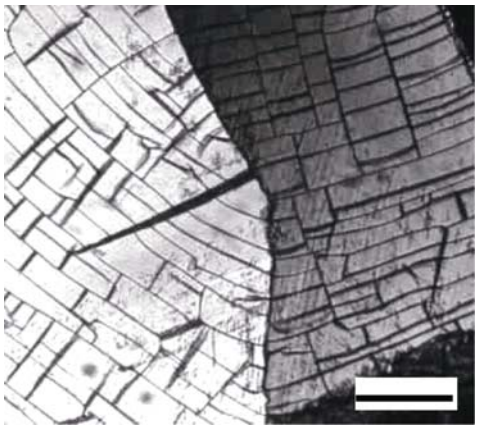

Figure 29 POM microstructure of the Nèel domain wall decorated by lamellae appearing in the mosaic-like morphologies of the CTV-2. The scale is 50 μm.

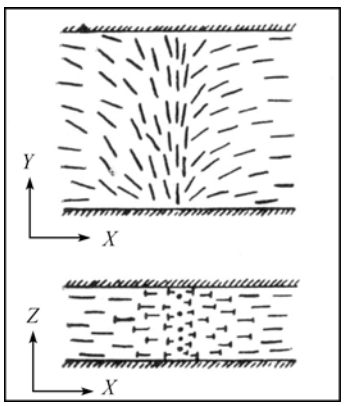

Figure 30 The illustration of director distribution around a Nèel domain wall.

The directors near the boundary are uncertain, therefore, the stress tends to concentrate, and more obvious cracks will be found（Figure 31）.

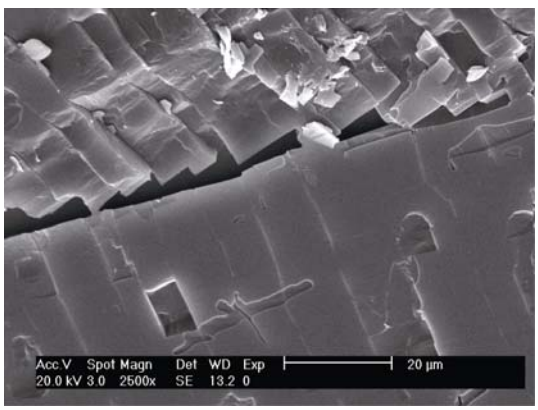

Figure 31 SEM microstructure of the Nèel domain wall decorated by lamellae appearing in the mosaic-like morphologies of the CTV-2.

3.4 The columnar nematic phase of bowlic molecules

The shapes of bowlic molecule and disk-like molecule are similar, so it is easy to misunderstand that the phase structures of both kinds of molecule are similar. All of them can form columnar phase indeed, however the nematic phase of disk-like molecule is generally regarded as random distribution of disks with only one direction orientation, and as shown in Figure 32(a), no column of disks exists. Only in hexagonal phase or tetragonal phase, the disks form columns (Figure 32(b) and (c)). The nematic phase of disk-like molecule is called D_N phase or N_D phase.[29]

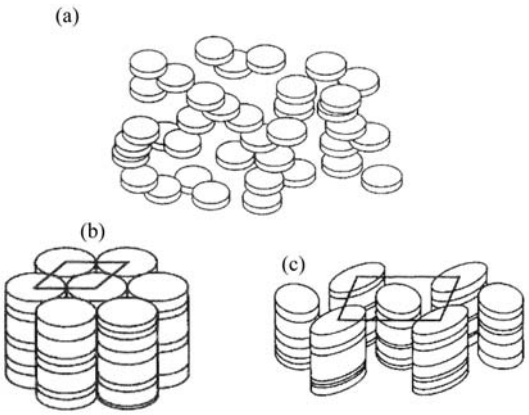

Figure 32 The illustration of the three kinds of liquid crystalline phases for disk-like molecules. (a) Nematic phase; (b) hexagonal phase; (c) tetragonal phase.

No detailed researches of phase structure of bowlic molecule have been found in literature. Therefore, according to the similarity of the shapes of bowlic molecule and disk-like molecule, the nematic phase of bowlic molecule (B_N) could be easily imagined as that shown in Figure 33. Nevertheless, we believe that the molecular columns occur in bowlic nematic phase. The reason is that bowlic molecules miss the up-and-down symmetry, and structure order will be higher[29]. Its driving force of forming a column is much stronger than that of disk-like molecules. Therefore, the liquid crystalline behavior of bowlic molecule is special, and bowlic molecular columns exist not only in hexagonal phase and tetragonal phase, but also in nematic phases. Figure 34 illustrates the structure of this special bowlic columnar nematic phase. In unoriented state, the bowlic molecular columns only have preferred orientation within every domain, but in oriented state, all of the bowlic molecular columns have preferred orientation, and the arrow represents the preferred direction of director. Figure 34 looks like the structure of a normal nematic phase, however the structure unit of bowlic nematic phase is different from that of normal nematic actually. The latter is simple rod-like molecule, however the former is bowlic molecular column, i.e. each bowlic molecular column acts as a normal rod-like molecule.

Figure 33 The nematic structure of bowlic molecules as an imitation of that of disk-like molecules.

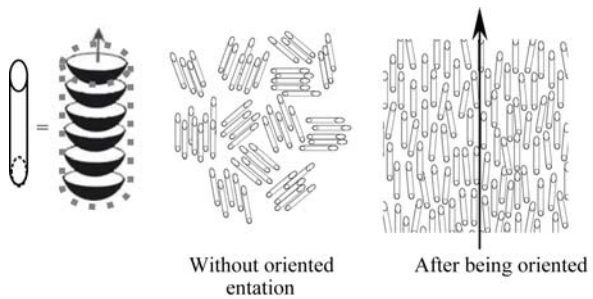

Figure 34 The illustration of the columnar nematic phase of bowlic molecules (B_{CN}).

Because there is only a limited number of researches concerned with liquid crystal phases of bowlic molecule, no system classification and nomenclature of them are found. Here we use B_{CN} to represent the bowlic columnar nematic phase, in order to distinguish from both normal nematic phase N and disk-like nematic phase D_N.

4 Conclusions

The special mosaic-like morphologies of bowlic CTV derivative molecules are the optical pattern of cracks initiated by the shrinking, because of the crystallization of frozen texture of nematic phases. The mosaic-like morphologies consist of lamellae, with each mosaic being a rectangular multi-layer lamella, which was composed by packed single layer lamella. The fibrils with the diameter of about 1 μm were observed directly, which were the structural units of lamella and would be

the bundles of the bowlic molecular columns. By means of the mosaic-like morphologies decoration technique, point disclinations such as $s = +1$ and $s = \pm 1/2$ and Nèel domain walls, which were very similar to normal nematic phase, were revealed in the novel bowlic molecular columnar nematic phase.

1 Lin L. Bowlic liquid crystals. Mol Crys Liq Crys, 1987, 146: 41－54[DOI]
2 Lin L. Liquid crystalline phase and molecular dimension. Physics (in Chinese), 1982, 11(3): 171－178
3 Zimmermann H, Poupko R, Luz Z, Billard J. Pyramidic mesophases. Z Naturforsch Teil A: Phys Phys Chem Kosmophys, 1985, 40A(2): 149－160
4 Malthête J, Collet A. Liquid crystals with a cone-shaped cyclotriveratrylene core. Nouv J Chim, 1985, 9(3): 151－153
5 Collet A. Cyclotriveratrylenes and cryptophanes. Tetrahedron, 1987, 43 (24): 5725－5759[DOI]
6 Dalcanale E. In: Lehn J M, ed. Comprehensive Supramolecular Chemistry. Vol 10, Chapt 20. New York: Pergamon, 1996
7 Lindsey A S. The structure of cyclotriveratrylene (10,15-dihydro-2,3, 7,8,12,13-hexamethoxy-5H-tribenzo [a, d, g]cyclononene) and related compounds. J Chem Soc, 1965, 1685－1692
8 Hyatt J A. Octopus molecules in the cyclotriveratrylene series. J Org Chem, 1978, 43(9): 1808－1811[DOI]
9 Collet A, Gottarelli G. Circular dichroism and absolute configuration of C3-chiral derivatives of cyclotriveratrylene. J Am Chem Soc, 1981, 103: 5912－5913[DOI]
10 Collet A, Gabard J. Optically active (C3)-cyclotriveratrylene-d9. Energy barrier for the "crown to crown" conformational interconversion of its nine-membered-ring system. J Org Chem, 1980, 45: 5400－5401[DOI]
11 Canceill J, Collet A, Gottarelli G. Optical activity due to isotopic substitution. Synthesis, stereochemistry, and circular dichroism of (+)-and (−)-[2,7,12-2H3] cyclotribenzylene. J Am Chem Soc, 1984, 106: 5997－6003[DOI]
12 Canceill J, Collet A. Exciton approach to the optical activity of C3-cyclotrylene derivatives. J Am Chem Soc, 1985, 107: 1299-1308[DOI]
13 Malthete J, Collet A. Ineversion of the cyclotribenzylene cone in a columnar mesophase: A potential way to ferroelectric materials. J Am Chem Soc, 1987, 109: 7544－7545[DOI]
14 Costante J, Garcia C, Collet A. Key intermediates in cyclotriveratrylene chemistry: A new route to the enantiomers of C3-cyclotriphenolene and cryptophane-C. Chirality, 1997, 9: 446－453[DOI]
15 Lutz M R, Zeller M, Becker D P. Beckmann rearrangement of cyclotriveratrylene (CTV) oxime: Tandem Beckmann-electrophilic aromatic addition. Tetrahedron Lett, 2008, 49(34): 5003－5005[DOI]
16 Westcott A, Fisher J, Harding L P, Rizkallah P, Hardie M J. Self-assembly of a three-dimensional triply interlocked chiral [2]catenane. J Am Chem Soc, 2008, 130(10): 2950－2951[DOI]
17 Ronson T K, Fisher J, Harding L P, Hardie M J. Star-burst prisms with cyclotriveratrylene-type ligands: A $[Pd_6L_8]_{12}^{+}$ stella octangular structure. Angew Chem Int Ed, 2007, 46(47): 9086－9088[DOI]
18 Sumby C J, Hardie M J. Capsules and star-burst polyhedra: An $[Ag_2L_2]$ capsule and a tetrahedral $[Ag_4L_4]$ metallosupramolecular prism with cyclotriveratrylene-type ligands. Angew Chem Int Ed, 2005, 44(39): 6395－6399[DOI]
19 Lunkwitz R, Tschierske C, Diele S. Formation of smectic and columnar liquid crystalline phases by cyclotriveratrylene (CTV) and cyclotetraveratrylene (CTTV) derivatives incorporating calamitic structural units. J Mater Chem, 1997, 7: 2001－2011[DOI]
20 Zimmermann H, Bader V, Poupko R. Mesomorphism, isomerization, and dynamics in a new series of pyramidic liquid crystals. J Am Chem Soc, 2002, 124: 15286－15301[DOI]
21 Ahmad R, Hardie M J. Synthesis and structural studies of cyclotriveratrylene derivatives. Supramol Chem, 2006, 18(1): 29－38[DOI]
22 Chen S X, Huang Y. Texture and defect of polymer liquid crystal state. In: Yang Y L, Hu H J, eds. Polymer Physics, Chapter 4 (in Chinese). Beijing: Chem Indus Press, 1991. 60－63
23 Windle A H, Dong Y, Lemmon T L, Spontak R J. Electron microscopy of thermotropic liquid crystalline polymers. In: Saegusa T, Higashimura T, Abe A, eds. Frontiers of Macromolecular Science. Oxford: Blackwell, 1989. 343－348
24 Dong Y M, Deng H Y. Morphological studies on varied nematic textures of aromatic copolyester B-N. Acta Polym Sinica (in Chinese), 1991, (5), 584－593
25 Qian R, Chen S. Band texture formation of sheared polymeric liquid crystalline state. Makromol Chem Macromol Symp, 1992, 53, 345－354
26 Wang W, Lieser G, Wegner G. Lyotropic liquid crystals of a soluble polydiacetylene. A comparative investigation by means of optical and electron microscopy. Liq Crys, 1993, 15(1): 1—24[DOI]
27 Gilles V, Jean-Pierre D, Galina M. Synthesis of C3-cyclotriveratrylene ligands for iron (Ⅱ) and iron (Ⅲ) coordination. Tetrehedron, 1995, 51(2): 389－400[DOI]
28 Canceill J, Collet A, Gottarelli G. (C3)-tris-(*O*-allyl)-cyclotriguaiacylene, a key intermediate in cyclotriveratrylene chemistry. Short and efficient synthesis of cyclotriguaiacylene. J Chem. Soc, Chem Commun, 1983, 122－123
29 Zhou Q F Wang X J. Liquid Crystal Polymers (in Chinese). Beijing: Academic Press, 1994. 9－10